Genetics: Published Articles Ahead of Print, published on November 1, 2004 as 10.1534/genetics.104.031930

Analysis of conditional paralytic mutants in *Drosophila* SERCA reveals novel mechanisms for regulating membrane excitability

S. Sanyal[*], C. Consoulas[†], H. Kuromi[‡], A. Basole[§, 1], L. Mukai[*], Y. Kidokoro[‡], K. S. Krishnan[§,††] and M. Ramaswami[*]

[*]MCB Department, Life Sciences South, University of Arizona, Tucson, AZ 85721, [†]Department of Experimental Physiology, Medical School, University of Athens, Greece, [‡]Institute for Behavioral Sciences, Gunma University School of Medicine, 3-39-22 Showa-machi, Maebashi, Japan, [§]Department of Biological Sciences, Tata Institute of Fundamental Research, Colaba, Mumbai 400005, India, and [††]National Center for Biological Sciences, GKVK Campus, Bangalore, 560 065, India.

[1] Pre**se**nt address: Department of Neurobiology, Duke University Medical Center, Durham, NC.

Running head: SERCA regulates neuromuscular physiology

Keywords: calcium/*Drosophila*/ ion channels /neuromuscular junction/ SERCA

Corresponding Author: Mani Ramaswami, Department of Molecular and Cellular Biology, 1007 E. Lowell Street, Life Sciences South, Box 210106, University of Arizona, Tucson, AZ 85721, USA. Tel: 1(520)621 6239. Fax 1(520) 6213709. Email: mani@u.arizona.edu

ABSTRACT

Individual contributions made by different calcium release and sequestration mechanisms to various aspects of excitable cell physiology are incompletely understood. SERCA, a sarco-endoplasmic reticulum calcium ATPase, being the main agent for calcium uptake into the ER, plays a central role in this process. By isolation and extensive characterization of conditional mutations in the *Drosophila* SERCA gene, we describe novel roles of this key protein in neuromuscular physiology and enable a genetic analysis of SERCA function. At motor nerve terminals, SERCA inhibition retards calcium sequestration and reduces the amplitude of evoked excitatory junctional currents. This suggests a direct contribution of store-derived calcium in determining the quantal content of evoked release. Conditional paralysis of SERCA mutants is also marked by prolonged neural activity driven muscle contraction, thus reflecting the phylogenetically conserved role of SERCA in terminating contraction. Further analysis of ionic currents from mutants uncovers SERCA-dependent mechanisms regulating voltage-gated calcium channels and calcium-activated potassium channels that together control muscle excitability. Finally, our identification of dominant loss-of-function mutations in SERCA indicates novel intra and inter-molecular interactions for SERCA *in vivo*, overlooked by current structural models.

INTRODUCTION

In neurons and muscles, local calcium transients control activities of proteins that directly mediate physiological processes such as transmitter release and contraction. Different pools of calcium, acting over longer time scales, may also modulate a variety of properties of excitable cells including action potential generation and transmitter responsiveness. Thus, the function of calcium release or sequestration mechanisms that regulate rapid or longer lasting calcium transients is of great importance (BERRIDGE *et al.*).

In neurons, calcium entry through voltage-gated channels tightly couples an action potential with transmitter release (CATTERALL; KATZ and MILEDI; SHENG *et al.*). In muscles, calcium entry, through ligand-gated channels, is the key to excitation-contraction coupling (MELZER *et al.*). Once calcium has entered the cell, it promotes the release of calcium from intra-cellular stores in the endo(sarco)plasmic reticulum (ER or SR). This calcium-induced-calcium-release (CICR), synchronously augments levels of cytosolic calcium and depends on the gating of ryanodine receptors located in the SR membrane (FABIATO; GYORKE *et al.*). In neurons and muscles, removal of calcium by either pumping it out of the cell or sequestering it into intra-cellular stores, restores cells to their resting state.

In addition to cytosolic calcium buffering proteins (ROBERTS) a significant contribution to intracellular calcium sequestration is made by membrane-bound calcium pumps that hydrolyze ATP to pump calcium either across the plasma membrane or into the ER/SR, the predominant store of intracellular calcium (BERRIDGE *et al.*). The

importance of sarco-endoplasmic reticulum calcium ATPases (SERCA) in regulating excitability is most clearly demonstrated by the unexpected observation that genetic knockout for phospholamban, a SERCA inhibitor peptide, cures several mouse models of cardiac dysfunction (MINAMISAWA *et al.*). Despite its importance, the contribution of SERCA to major aspects of neuromuscular physiology remains poorly understood. Most significantly, the relative importance of SERCA-dependent mechanisms in calcium sequestration and/or signaling has not been assessed critically. Even in cardiac disease where SERCA dysfunction has been implicated (GOMMANS *et al.*; HASSELBACH; LOKE and MACLENNAN; ODERMATT *et al.*) the precise physiological underpinnings of these effects remain to be elucidated.

Here, we report the isolation of conditional mutations in the *Drosophila* SERCA gene (dSERCA, *Ca-P60A*), and the first detailed genetic analysis of the effects of SERCA inhibition on neuromuscular physiology. Since *Drosophila* neurons and muscles function by mechanisms largely similar to those in vertebrates (SUZUKI and KANO), these findings are likely to be broadly applicable. Our observations indicate the existence of a) hitherto uncovered molecular interactions important for SERCA function *in vivo*, b) SERCA-dependent mechanisms that contribute substantially to control of calcium pools at the presynaptic motor terminal and c) SERCA-dependent modulation of ionic currents that regulate muscle contraction and excitability. Although pharmacological perturbation of SERCA function has been extensively used for various studies (TOYOSHIMA *et al.*), our results compliment and significantly extend previous findings. They also offer avenues for the genetic analysis of store calcium function and provide fundamental new insight into SERCA functions *in vivo*.

MATERIALS AND METHODS

Drosophila stocks and culture:

The Canton-Special (CS) strain was used as the wild-type in the present study. The EP lines were a part of the Pernille Rorth collection (RORTH); deletions were obtained from the *Drosophila* Stock Center, Bloomington, Indiana. Other dSERCA alleles and the genomic rescue construct for dSERCA were from G. Periz (PERIZ and FORTINI). The rescue construct contains the entire genomic region for dSERCA with all the introns and 4-5 Kb of DNA on either side of the gene. All other *Drosophila* strains are a part of the TIFR or Ramaswami laboratory stock collection. Flies were reared on standard cornmeal-dextrose-yeast medium at 22-25^{o}.

EMS mutagenesis and screening:

For the mutagenesis, ethylmethane sulfonate(EMS), a chemical mutagen which mostly induces point mutations was used. Two to three day old Canton-S (CS) males were starved for 6 hours and introduced into bottles containing filter paper discs soaked in 0.75% EMS in 2% sucrose. The males were allowed to feed for 12 hours and mated to virgin CS females. A total of 200,000 F1 progeny were screened for paralysis at 40^{o}. Any fly that paralyzed within three minutes was picked as a putative mutant and used to set up a mutant line by crossing to suitable males or virgins.

Behavioral assays:

The apparatus used for measurement of adult paralysis, the Sushi Cooker, has been described before (RAMASWAMI *et al.*). Paralysis was empirically defined as the

condition where the animal lies on its back with little effective movement of the legs and wings. All flies tested were one to two days old. We define the restrictive temperature for all the behavioral analyses as the temperature at which 100% flies paralyze in three minutes. Paralysis profiles were obtained by introducing 10 flies at a time in the cooker, and recording the number of flies immobile at fixed intervals of time. Each data point represents the mean from three such runs.

Lethality staging:

Sibling crosses between heterozygous *Ca-P60A*$^{Kum170/}$+ and *Ca-P60A*$^{Kum295/}$+ were set up for lethality staging. In this cross, 25% of the progeny is homozygous for the *Ca-P60A* mutation and are expected to be lethal. The initial number of eggs laid was counted and the bottles were incubated at 25^{o} for 24 hours at the end of which the number of unhatched eggs was determined. After a further incubation period of 30 hours, the number of second instar larvae was determined. The stage of lethality was defined as the point where the expected 25% lethality was observed. For each genotype, the data is averaged over five experiments, each consisting of at least 200 embryos. For determining the embryonic stage of death, freshly laid eggs were covered with halocarbon oil and observed under an inverted microscope throughout embryogenesis till hatching.

Recombination, deletion mapping, sequencing and homology modeling:

A set of EP lines from the Pernille Rorth collection was used as second chromosome markers. *w*; *CaP60A*^{Kum170}/ *CyO* females were crossed to *w*; EP/ *CyO* males from various lines. The *w*; *CaP60A*^{Kum170}/ EP progeny females were further crossed to *w*;

CyO/ *Tft* males. All *Cy* progeny was screened at 40^{o} for three minutes, to assay for the presence of the *CaP60A*^{Kum170} mutation and scored for the w^{+} marker carried by the P-element. Recombination frequency was calculated as- Number of recombinants/ Total number of flies X 100. At least 100 flies were screened for each EP line. About 500 flies were screened for the three lines closest to *CaP60A*^{Kum170}, EP938, EP348 and EP540.

For deletion analysis, various chromosomal deletions were tested for their ability to uncover the recessive lethal phenotype of *CaP60A*^{Kum170}. *CaP60A*^{Kum170}/ *CyO* flies were crossed to flies carrying a specific deletion balanced over the *CyO* balancer chromosome. The progeny was screened for the presence of non-*Cy* flies. A total absence of non-*Cy* flies indicates that the mutation lies in the region that is deleted in a particular deficiency line.

The fly SERCA was homology modeled using Swiss-Model (www. expasy.org/swissmod/SWISS-MODEL.html) on the reported rabbit SERCA crystal structure (TOYOSHIMA *et al.*) using standard parameters. *Drosophila* SERCA shares a high degree of homology with various vertebrate isoforms (~ 70%).

Generation of the *CaP60A*^{KumP52} allele and excision analysis:

To generate a P element tagged allele of *CaP60A, w/w*; EP938/*CyO* females were crossed to males from a line containing a source of the transposase, *w*/ Y; (Δ2-3)*Sb*/ TM6(*Tb*) to generate the "jump starter" flies. The jump starter males were further crossed to *w/w*; *CaP60A*^{Kum170}/*CyO* virgin females. 1400 lines were set from the *Cy* progeny by crossing individual males, with a mobilized EP938 balanced over *CyO*, to *w*; *CaP60A*^{Kum170}/*CyO* virgin females. The progeny of these lines were screened for the

absence of non-*Cy* flies. For excising the P-element from the *CaP60A* locus, *w*; *CaP60A*$^{Kum\text{P52}}$/ *CyO* females were mated to *w*;/Y; +/ *CyO*; (Δ2-3)*Sb*/ + males and the F1, *w*/Y; *CaP60A*$^{\text{KumP52}}$/ +; (Δ2-3)*Sb*/+ male progeny was collected. These males were further crossed to *w*; *CaP60A*^{Kum170}/ *CyO* females. All *CyO* progeny was screened for the presence of non-*Sb*, white-eyed males, in which the P element would have excised out. Such males were individually crossed to *w*; *CaP60A*$^{\text{KumP52}}$/ *CyO* females and the lines were screened for reversion of the lethal phenotype.

Plasmid rescue:

The EP transposable element in these flies allows plasmid rescue of flanking fly genomic DNA using the single *Eco*RI restriction site in the vector. Genomic DNA was isolated from *CaP60A*$^{\text{KumP52}}$ flies and restricted with *Eco*RI using standard procedures. The DNA was ligated overnight and used for transformation of competent *E. coli*. Colonies transformed with the rescued DNA fragment were analyzed by RFLP analysis. Flanking genomic DNA from an *Eco*RI-*Kpn*I fragment was sequenced using automated sequencing. A BLAST search of the sequence was carried out using the BLASTn program at NCBI.

Generation of antibodies against dSERCA peptides and immuno-histochemistry:

Two 20 amino acid stretches were selected from the dSERCA protein. The first, SS1 (ERGLTLDQIKANQKKYGPNE) is from a.a. 21 to a.a. 40 and the second peptide SS2 (TLKFVARKIADVPDVVVDRM)is from a.a. 983 to a.a. 1002. Generation of antibodies including peptide synthesis, conjugation to KLH and affinity purification was

carried out by Alpha Diagnostics Intl. Inc. (5415, Lost Lane, San Antonio, TX 78238, USA, http://www.4adi.com). Antibody titer was monitored after each booster immunization. The final bleeds were affinity purified and used at a concentration of 1:1000 for immuno-histochemistry and 1:10,000 for western blotting. For immunohistochemistry, larvae were dissected in calcium-free HL3 saline, fixed in 4% paraformaldehyde and stained overnight in blocking solution containing 0.1% Triton X-100. Mouse anti-BiP (anti-KDEL, StressGen SPA-827) was used at 1:100. All secondary antibodies were Alexa dye conjugated anti-rabbit and anti-mouse antibodies from Molecular Probes. Protein gels and western blotting were according to standard procedures (LAEMMLI and QUITTNER) and as per manufacturer's instructions (Amersham).

Electrophysiology :

Adult DLM recordings: Intracellular recordings were made from the DLM e, f muscle fibers (COSTELLO and WYMAN; IKEDA and KOENIG; KING and WYMAN). Intact adults were immobilized on wax and a small hole was made in the dorsal part of the thorax where DLM e,f muscle fibers are positioned. Glass microelectrodes of 10 to 20 MΩ resistance were used to record the muscle potentials. Muscle stimulation was achieved by activating the DLM e,f motoneuron (MN5) through the giant fiber system (GFS; (THOMAS and WYMAN)). GFS was stimulated by a tungsten electrode placed in the eye of the fly.

Larval current recordings: Calcium current recordings were made as described previously (GIELOW *et al.*). Recording saline to block all potassium currents contained

(in mM): NaCl (77.5), KCl (5), $MgCl_2$ (4), $NaHCO_3$ (2.5), trehalose (50), sucrose (115), Hepes (5), tetra-ethylammonium (TEA) (20), 4-aminopyridine (4-AP) (1), quinidine (0.1), and $BaCl_2$ (10). All currents were Barium currents through voltage-gated calcium channels. For measurement of calcium activated potassium currents (slowpoke currents), recordings were done in normal HL3 medium with 100 mM Ca[2+] and 2 mM 4-AP to block the fast Shaker potassium current (I[A]). Voltage steps were in increments of 10 mV from a holding potential of –70 mV. The slowpoke current could be most clearly discerned at a voltage step to 0 mV, where there is maximal calcium current and the slower potassium currents are minimal (ELKINS *et al.*). This current could be completely suppressed by removing calcium from the recording medium. The currents were not normalized with capacitance measurements since all recordings were from muscle 6 in abdominal segment 2 of separate animals. Muscle surface areas were independently confirmed to be similar. The resting membrane potential was determined at the end of each voltage clamp experiment and only traces from animals with resting potentials more negative than –50mV were included in the analysis. Traces were digitally leak subtracted and baseline adjusted for analysis. Representative traces are plotted using the electrophysiology module in SigmaPlot (Jandel Scientific).

Larval EJC recordings: EJC recordings were made in HL3 saline (STEWART *et al.*) with 1mM Ca[+] as described previously (SANYAL *et al.*). All recordings were made from muscle 6 in segment A2 of wandering third instar larvae. Muscles were voltage clamped at –70mV, and excitatory junctional currents were evoked, by stimulating the segmental nerves such that both neurons innervating muscle 6 were recruited. The nerves were stimulated at 0.5 Hz and a train of 25 stimuli were averaged for each recording. For

spontaneous events, a one-minute continuous recording was used to determine mEJC amplitude and frequency. The traces were analyzed using the mini-analysis software (synaptosoft inc.).

Calcium imaging at the larval NMJ:

The preparations were incubated for 40 minutes in nominally zero Ca^{2+} saline ($CaCl_2$ was replaced with 2 mM $MgCl_2$ in normal saline) containing 10 μM rhod-2/AM, 0.03% pluronic F-127 in the dark at 22^{o}. The preparation was rinsed with HL3 medium three times. The fluorescence was excited at 545 nm and monitored at wavelengths above 580 nm. To excite nerve terminals, pulses (1 ms and 2x threshold voltage) were delivered to the appropriate segmental nerve via a conventional glass suction electrode (20-30 μm inside diameter).

RESULTS

Isolation of conditional *Kum* mutants and their behavioral phenotypes:

Two independent mutant lines isolated in our screen for temperature-sensitive paralytic mutants showed identical dominant paralytic behavior at 40^{o} (Materials and methods). Both mutations were localized to the second chromosome and were recessively lethal. Genetic recombination analysis showed that the dominant paralytic phenotype co-segregated with the recessive lethal phenotype. The two mutations *170* and *295*, were tentatively classified as allelic, because they not only mapped to the same chromosomal region, but also did not complement for the recessive lethal phenotype. Thus, the mutants were named *Kumbhakarna*^{170} (*Kum*^{170}) and *Kumbhakarna*^{295} (*Kum*^{295}). The conditional paralytic behavior of *Kum*^{170}/+ and *Kum*^{295}/+ heterozygous flies are documented in Figure 1A. The mutants, but not wild-type controls, paralyze at 40^{o} within three to five minutes. When restored to permissive temperatures (20^{o}), paralysis persists for 6 to 48 hours depending on the duration of prior exposure to restrictive temperature. (This prolonged inactive phase, unique among *Drosophila* t.s paralytics, led to the gene being named after an eponymous mythological hero who slept for 6 months of the year). The prolonged recovery phase might derive from irreversible heat-sensitive alteration of the mutant protein or from chronic effects on membrane excitability (see later sections).

Like adults, *Kum* larvae are also paralyzed at 40^{o} within five minutes; paralyzed *Kum* larvae appear shortened due to severe contraction of the body wall musculature (Figure 1B). This observation suggested a role for the *Kum* gene product in suppressing muscle contraction. Consistent with this, many homozygous *Kum*^{295}/*Kum*^{295} mutant

embryos also appeared abnormally contracted inside the egg case (Figure 1C), although most *Kum*^{170}/ *Kum*^{170} animals developed normally and hatched into very sluggish first-instar larvae.

To distinguish between two possibilities, whether *Kum* mutations prolonged nerve-evoked muscle contraction or induced spontaneous muscle contraction, we examined *Kum* phenotypes in a *para*^{ts} background that allows conditional inactivation of neuronal voltage-gated Na channels encoded by the *para* locus (LOUGHNEY *et al.*). In *para*^{ts1}*; Kum* double mutants, the characteristic contraction of *Kum* mutants was completely abolished so long as *para* dependent nerve transmission was blocked (Figure 1D). Conversely, at temperatures permissive for *para*, previously heated *Kum* mutants contracted as expected. Together, these data indicate a need for the *Kum* gene product in neuromuscular function; specifically in limiting the duration of neurally evoked muscle contraction.

Kum mutants have mutations at the dSERCA locus:

Recombination mapping, using a set of independent, *white* marked P-element inserts from the Pernille Rorth EP collection, placed *Kum* in the cytological interval 59A-60E, at the tip the right arm of the second chromosome. An analysis using overlapping deletions in this region (Figure 2A) further narrowed the location to the 60A1-B1. To clone the *Kumbhakarna* gene, the EP938 transposon, which is located at 59F6-8 on the second chromosome, was mobilized in order to disrupt the *Kum* locus at 60A1-B1 (Materials and Methods). A lethal line generated from this mobilization, P52, failed to complement the lethality of *Kum*^{170}, *Kum*^{295} or a chromosomal deficiency in the region,

Df(2R)bw-S46. The phenotypes of this mutant line mapped to *Kum*, and were caused by a P-element insertion as evidenced by successful and frequent reversion of all mutant phenotypes by remobilization of the P-transposon (Materials and Methods). This P-element induced lethal allele has been named Kum^{P52}. This allele does not display temperature sensitive paralysis like the EMS induced alleles and is probably a hypomorphic allele. Genomic DNA flanking the P52 insertion was recovered and, when sequenced, found to be identical to the upstream regulatory region of the organellar type Ca^{2+} ATPase gene in *Drosophila* (*dSERCA*, *CaP60A*) (MAGYAR *et al.*). The location of the P-element in the genome of the Kum^{P52} flies is shown in Figure 2A. The P-element separates the upstream regulatory elements of the gene from the TATA box and the coding region.

To confirm that the mutant phenotypes resulted from altered SERCA function we ensured first that the *Kum* alleles did not complement recently described EMS-induced dSERCA lethals (PERIZ and FORTINI), and second that the mutants carried lesions in the Ca^{2+}-ATPase gene. In addition to non-complementation observed between our *Kum* alleles and *bonafide* Ca^{2+}-ATPase mutations, we discovered that one of the previously reported recessive lethal alleles, $CaP60A^{l1}$ displays dominant paralytic phenotypes identical to Kum^{170} and Kum^{295} (henceforth called $CaP60A^{Kum170}$ and $CaP60A^{Kum295}$ respectively). Further sequence analysis revealed that $CaP60A^{Kum170}$ and $CaP60A^{l1}$ carry single-base substitutions in *Drosophila* SERCA coding sequences, predicted to cause a Glu442 to Lys mutation ($CaP60A^{Kum170}$) or a Cys318 to Ser ($CaP60A^{l1}$) substitution in the sequence of SERCA (Figures 2A and B). The location of the two mutations is indicated on a homology modeled 3D dSERCA structure (see Materials and Methods). Both

mutations are located in the hinge domain and could potentially influence either ATP binding or conformational state of the molecule (TOYOSHIMA *et al.*). Together with the observation that the *CaP60A*^{Kum170} and *CaP60A*^{Kum295} recessive lethal phenotypes were completely rescued by a genomic transgene of dSERCA, these data establish that mutations at the dSERCA locus cause the phenotypes we observe in *Kum* mutants. We selected *CaP60A*^{Kum170} for further extensive analysis because of the robustness of the phenotypes, however, all phenotypes are exhibited by *CaP60A*^{Kum295} as well.

dSERCA is abundantly expressed in both neurons and muscle:

In order to visualize the distribution of the SERCA protein in flies, we raised antibodies against two carefully selected 20 amino acid peptides derived from the fly SERCA sequence (see materials and methods). After immunization the antibodies were affinity purified using immobilized peptide columns and were used in all experiments. The antibody recognizes the predicted SERCA band at about 100 KDa in western blots of total fly protein (1003 amino acids, Figure 3A). The pre-immune sera as well as antibody pre-adsorbed on free peptide failed to detect this band.

SERCA antibodies stain the body wall muscles strongly (Fig 3C). This is expected given that SERCA is known to form a large fraction of the total protein content of sarcoplasmic reticulum. The observed staining clearly highlights a membrane network (consistent with ER) that extends to the nuclear envelope (Fig. 3C, D). To further show that our antibodies to SERCA label the ER, we double stained larval body wall preparations with anti-SERCA and anti-BiP (StressGen, SPA-827), an antibody that labels KDEL containing proteins that are retained in the ER. Figure 3D clearly shows extensive

colocalization between SERCA and KDEL containing proteins, thus indicating that our antibody does indeed label SERCA in ER and nuclear membrane. The two lower panels in figure 3D are single planes at different depths through a muscle nucleus (shown using TO-PRO3 staining in blue) and further demonstrate the marked colocalization of an ER marker and SERCA. Neurons cultured from the ventral ganglia of wandering third instar larvae (KRAFT *et al.*) also stained positive for SERCA throughout the cell. (Fig.3B). These staining patterns, not seen with control preimmune serum, indicate that SERCA is highly expressed in intracellular membranes widely distributed through the cytoplasm of both neurons and muscles.

CaP60A^{Kum170} mutations are loss-of-function mutations in dSERCA:

Mutations in dSERCA are likely to cause impaired calcium sequestration. However, the selection criteria we used in isolation of the mutants could have led to specific recovery of unusual alleles that might, for instance, sequester calcium at a faster rate. To firmly interpret our mutant phenotypes in terms of SERCA function, we tested whether the mutant effects on presynaptic calcium were similar to those observed in response to treatment with thapsigargin, an established SERCA inhibitor in vertebrates. The effect of thapsigargin has also been most simply and conclusively shown in *Drosophila* at the presynaptic nerve terminal (KUROMI and KIDOKORO). Hence, we used this assay to test the effect of our mutations in altering calcium dynamics in this paradigm.

At wild-type larval motor terminals, presynaptic calcium levels, assessed using Rhod-2 based calcium detection, are increased during a four minute burst of 30 Hz nerve stimulation (KUROMI and KIDOKORO). Within two minutes after cessation of stimulation,

calcium levels fall in wild type animals to a value that remains significantly elevated compared to pre-stimulus levels. In the presence of thapsigargin (Tg), the initial peak of calcium during stimulation is higher but after stimulation levels return to baseline rather than remain elevated. Together these data indicate that SERCA-dependent calcium sequestration limits the initial calcium peak and that release from internal stores contributes significantly to the sustained elevation of calcium observed following 30Hz stimulation. The return to baseline and lack of sustained high levels of calcium is possibly due to the subsequent depletion of internal stores (KUROMI and KIDOKORO).

At 22^{o} in both Canton-S controls and *CaP60A*^{Kum170}, the rhod-2 fluorescence intensity in boutons increased during stimulation at 30 Hz and declined gradually after tetanus but stayed at a slightly elevated level for a prolonged time (Figure 4A, *Kum*^{170}(unheated) and B, *Kum*^{170}(-heat), open circles with solid line, and CS (-heat), dotted line with open circles). In *CaP60A*^{Kum170} preparations treated with thapsigargin (20 uM for 20 minutes), the rhod-2 fluorescence intensity increased to a higher peak during early phase and declined during tetanus. After tetanus, the fluorescence rapidly declined to the pretetanus level (Figure 4A, *Kum*^{170} +Tg (unheated) and B, *Kum*^{170} +Tg, filled circles with solid line). These patterns are similar to those observed in wild type animals treated with Tg (KUROMI and KIDOKORO). When *CaP60A*^{Kum170} was exposed to 40^{o} for 15 minutes, the changes in rhod-2 fluorescence in boutons during and after tetanus showed the same patterns as those observed in *CaP60A*^{Kum170} treated with thapsigargin at 22^{o} (Figure 4A, *Kum*^{170}(heated) and B, *Kum*^{170}(+heat), solid line with triangles). CS animals, on the other hand, behaved similar to unheated CS controls and did not show either an initial peak nor a return to pretetanus levels (Figure 4B, CS(+heat), dotted line with

triangles). Thus, mutant *CaP60A*^{Kum170} animals showed conditional alterations in calcium handling similar to those observed in thapsigargin treated animals. In addition to establishing *CaP60A*^{Kum170} as a dominant loss-of-function allele of SERCA, these experiments serve to further establish that a SERCA-containing compartment and SERCA-dependent functions operate to control calcium dynamics in the presynaptic terminal.

Since the allele P52 does not have a paralytic phenotype, it is possible that the dominance of the loss-of-function alleles derives from a potentially oligomeric state of SERCA in the membrane. Thus, in these alleles, on heating, a majority of the oligomers are rendered non-functional, leading to paralysis. It is also possible that since in the dominant alleles, half the SERCA molecules on ER/SR membrane are mutant, heat inactivation would alter the overall efficacy of calcium sequestration in these animals. In the P52 allele, on the other hand, SERCA molecules derived from the wild-type copy of the gene on the other chromosome, might achieve "normal" density of functional SERCA molecules on the ER/SR membranes leading to normal function in the heterozygotes. Only in a homozygous condition is this allele lethal, probably owing to a critical reduction of SERCA molecules. A further consideration of this issue is provided in the discussions.

SERCA dependent mechanisms control quantal content of evoked presynaptic release:

Since our experiments showed that presynaptic calcium levels are acutely controlled through SERCA function, we tested the effect of SERCA inhibition on evoked release at the presynapse. Two-electrode voltage clamp recordings done at the

neuromuscular junction of untreated and treated wild type and *CaP60A*^{Kum170} third instar larvae show a significant reduction (about 50%) in evoked but not spontaneous release (Figure 5A and B). (Under voltage-clamp conditions, only the post-synaptic response to presynaptically released neurotransmitter is measured, without any contribution from the voltage-gated channels.) This change, not seen at wild-type nerve terminals treated similarly (40^{o} for five minutes, followed by recordings made at room temperature; WT at at room temperature, mean EJC amplitude is 40 +/- 3 nAmps, n = 10 and after heating 42 +/-2 nAmps, n = 8), is probably due to progressive depletion of calcium in the pre-synaptic compartment or to chronic inhibition of pre-synaptic calcium channels (see section on effects of SERCA inhibition on post-synaptic voltage-gated calcium channels). Thus, SERCA dependent calcium sequestration may contribute directly or indirectly in determining the number of vesicles that are released following depolarization of the nerve terminal. That there is no change in the mEJC size, indicates normal vesicle filling and post-synaptic receptivity.

SERCA permits repetitive muscle action potential generation by preventing attenuation of voltage-gated calcium currents:

Following our observation of complete wing immobility in paralyzed *CaP60A*^{Kum170} adults, we initially examined both spontaneous firing of the dorsal longitudinal flight muscles (DLM) and their response to stimulation of the giant fiber pathway (COSTELLO and WYMAN; IKEDA and KOENIG; KING and WYMAN). In wild-type animals, recordings of spontaneous activity in flight muscles reveal intermittent bursts of action potential firing in DLMs (Figure 6A top trace). These groups of action potential

spikes are thought to be representative of the flight pattern (IKEDA and KOENIG). A single "spike" is composed of a slow rising phase, the epsp (excitatory post-synaptic potential) representing response to released transmitter (glutamate) and a rapid action potential generated by the active responses of voltage-gated ion channels on muscle membrane. These characteristics are largely unchanged in unheated *CaP60A*^{Kum170} animals. In contrast, in recordings made at room temperature after a five minute exposure to 40°, *CaP60A*^{Kum170} DLMs showed characteristic broad multi-peaked action potentials progressing eventually to spike failure (Fig. 6A bottom traces).

To more carefully define the origin of this phenotype, we analyzed DLM responses elicited by controlled stimulation of the motor nerve. Frequencies up to 50 Hz were used to evoke action potentials. Wild type DLMs "follow" these stimulation frequencies with high fidelity. In contrast, untreated *CaP60A*^{Kum170} DLM fibers show frequent action potential failures at 30 Hz (Fig 6B, arrows in middle trace). That this phenotype derives from mutations at the dSERCA locus is further proved by the fact that in heat-exposed *CaP60A*^{Kum170} animals, failures are observed at even lower frequencies of about 10 Hz. At a given frequency of stimulation, failures are observed earlier in heated *CaP60A*^{Kum170} animals than in unheated *CaP60A*^{Kum170} animals (Fig. 6B, compare with arrows in bottom trace). The failures could derive either from defects in action potential generation in muscles or reduced pre-synaptic neurotransmitter release (leading to sub-threshold EPSPs that do not lead to spiking, arrowhead in Fig. 6B) or both.

Thus, we next tested if SERCA dependent mechanisms in muscle serve to regulate excitability and action potential generation. Action potentials in *Drosophila* muscle are initiated by voltage-gated calcium currents. Since we observed a high incidence of spike

failures in heated *CaP60A*^{Kum170} animals, we tested whether voltage-gated calcium currents in muscles are altered in *CaP60A*^{Kum170} mutants after heat exposure. Larval body wall muscles are particularly convenient and well-established for voltage-clamp analysis of calcium currents (GIELOW *et al.*). We specifically measured the voltage-gated inward calcium current (by blocking all potassium channels – see Materials and Methods) in heated and unheated *CaP60A*^{Kum170} animals. We find that voltage-gated calcium currents are dramatically and chronically reduced in heated *CaP60A*^{Kum170} animals (Figure 7A and B). In contrast, unheated *CaP60A*^{Kum170} animals show calcium currents that are comparable to wild type. This reduced voltage-gated calcium current can account completely for spike failure, even in the presence of normal excitatory post-synaptic potentials (EPSPs). Thus, under normal conditions, SERCA dependent calcium sequestration may serve to independently regulate the excitability of muscle by controlling signaling from intracellular stores of calcium that lead to inactivation of VGCCs.

SERCA mediated calcium sequestration influences muscle action potential waveform by modulating calcium activated potassium currents:

As mentioned before, spike failure in *CaP60A*^{Kum170} muscles is preceded in several instances by spike broadening (arrows in Figure 8A). Such a multi-peaked prolonged action potential has been described previously in *slowpoke* mutants (ATKINSON *et al.*; ATKINSON *et al.*). In these animals, a defect in the calcium-activated potassium channel encoded by the *slo* gene, results in a slower falling phase of an action potential. This is because the calcium-activated outward potassium current is abolished or reduced. In *CaP60A*^{Kum170} animals a potential mechanism by which this can happen is due to run down

of internal calcium stores that likely play an important role in activating the *slo* channels.

In addition to the broadening of spikes in *CaP60A*^{Kum170} animals, we also noticed that both the rising and falling phase of the action potential are slower. Figure 8B shows a comparison of the rise time and half decay time of consecutive action potential trains from wild type, *CaP60A*^{Kum170} unheated and *CaP60A*^{Kum170} heated animals. It is readily apparent that both the rise and decay are significantly slower in heated *CaP60A*^{Kum170} animals. Likely explanations for these phenomena derive from effects on the two predominant channels that contribute to these components of an insect muscle action potential. Rise times are influenced most acutely by alterations in the inward calcium current, and thus, a slow rise time could derive from the reduced voltage-gated calcium current. Similarly, the time for decay of the action potential is influenced by outward potassium currents. The observed increase in decay time could, therefore, derive from reduced calcium activated potassium currents.

To directly test if the calcium activated potassium currents are indeed reduced in *CaP60A*^{Kum170} animals, we measured the outward slowpoke current from larval muscles. This was done by recording currents under voltage clamp in normal ringer's solution containing 100 mM Ca[2+] and 2 mM 4-AP ((ELKINS *et al.*), materials and methods). Under these conditions a voltage step to 0mV elicited a robust calcium dependent outward current that represents the slo current. As seen in figure 8 C and D, slo currents are highly reduced in both unheated and heated *CaP60A*^{Kum170} animals. This correlates satisfactorily with the action potential broadening observed in both unheated and heated *CaP60A*^{Kum170} animals and gives an accurate estimate of the state of cytosolic calcium in these larvae. Thus, SERCA dependent maintenance of store calcium is critical for normal activation of

slowpoke channels and recovery during repetitive action potentials.

Impairment of dSERCA function in muscles is sufficient to phenocopy the *CaP60A*^{Kum170} mutations:

Since SERCA is found at high levels in both neurons and muscle and impairment of SERCA function results in both neural and muscle phenotypes, it is conceivable that the conditional paralytic phenotype in *CaP60A*^{Kum170} mutations derives from defective SERCA function in both these tissues. To determine neural and muscular contributions to the paralytic phenotype of SERCA mutants, we made use of the GAL4-UAS system (BRAND and PERRIMON) and cloned the mutated SERCA cDNA from *CaP60A*^{Kum170} into the pUAST vector (materials and methods). We further generated flies carrying this transgene (UAS-*CaP60A*^{Kum170}) and crossed them to GAL4 lines that drove expression from *UAS- CaP60A*^{Kum170} in neurons, muscles or both tissues (Table 1). The effect of driving this dominant negative SERCA protein was assayed by a simple test for paralysis at restrictive temperatures.

Neural expression of *CaP60A*^{Kum170} using elav^{C155} (pan-neural), cha (cholinergic neurons) or C380 (predominantly motor neurons) GAL4 drivers did not cause any observable paralysis at restrictive temperatures. Amplified expression in all neurons using elav^{C155}; UAS-GAL4 (HASSAN *et al.*) also proved to be ineffective at causing behavioral paralysis. Thus, while SERCA function in neurons is likely to be important, a disruption of this function via *CaP60A*^{Kum170} overexpression is not sufficient to lead to dominant paralysis.

In a different set of experiments, we used three ubiquitous GAL4 drivers (*arm-*

GAL4, *tubulin-GAL4* and *shi-GAL4*) and three muscle drivers (*MHC-GAL4*, *24B-GAL4* and *mef2-GAL4*. While *tubulin-GAL4* and *24B–GAL4* animals showed larval paralysis, *mef2 GAL4* animals showed both larval and adult paralysis completely undistinguishable from that in $CaP60A^{Kum170}$ (Table 1). Taken together, these observations clearly suggest that strong expression of mutant dSERCA protein in muscles, that probably alters the relative stoichiometry of wild-type versus mutant SERCA molecules, is necessary and sufficient to duplicate the mutant paralytic phenotype and further tighten the causal link between mutations in the SERCA gene and observed phenotypes.

Mef-2 (*m*yocyte *e*nhancer *f*actor-*2*) is a transcription factor that is absolutely necessary for the proper development and differentiation of all classes of *Drosophila* musculature. A scan of the upstream region of the Ca-P60A gene for conserved transcription factor binding sites revealed two closely spaced, highly conserved binding sites for Mef-2. The first site occurs between 465-474 (ggttTAAAaa) and the second site occurs between 481-490 (tttcTAAAta) 5' from the transcription start site. Both the sites occur on the plus strand and have a score of 1 for the conserved core sequence (PromoterInspector program at Genomatrix). It is conceivable that the spatio-temporal pattern of expression of dMef-2 also determines the physiologically relevant accuracy of SERCA expression and hence, mef-2-GAL4 is the most potent in replicating the dSERCA mutant phenotypes.

To conclusively test if electrophysiological defects observed in muscles of $CaP60A^{Kum170}$ mutants are present in the *mef2-GAL4; UAS-*$CaP60A^{Kum170}$ animals, we recorded spontaneous and evoked responses from DLMs of both heated and unheated *mef2-GAL4, UAS-* $CaP60A^{Kum170}$ flight muscles. As shown in figure 9A and B, it is clear

that DLM firing in *mef2-GAL4, UAS- CaP60A*^{Kum170} animals is qualitatively similar to that in *CaP60A*^{Kum170} mutants. Thus, genetically mosaic animals with wild-type nervous systems but SERCA-mutant muscle, show all defects in flight muscle physiology characteristic of *CaP60A*^{Kum170} mutants in both spontaneously firing (Figure 9A) and giant fiber stimulated (Figure 9B) recordings (arrow marks failures and arrowhead indicates presence of robust EPSPs). In control experiments, none of these effects are observed in either the *mef2-GAL4* line or the *UAS- CaP60A*^{Kum170} line alone (data not shown). These results suggest that the behavioral phenotype of temperature-sensitive paralysis in *CaP60A* mutants is predominantly, if not wholly, a consequence of SERCA inhibition and altered excitability in muscle.

DISCUSSION

Cellular calcium dynamics are subject to stringent spatio-temporal control, especially in excitable cells. While the role for intra-cellular stores of calcium in this context is generally held to be important, details of how these stores may modulate the functioning of neurons and muscles are incompletely understood. SERCA is a key player in regulating intracellular calcium and its physiological effects as underscored by the observation that SERCA dysfunction underlies several different forms of cardiac disease (GOMMANS *et al.*). In representative animal models of cardiac disease while impairment of SERCA activity has been shown to cause arrhythmic contraction, mechanisms by which SERCA affects electrical properties of cardiac cells remain incompletely described.

Although pharmacological perturbation of SERCA in other model systems using relatively specific drugs such as thapsigargin and cyclopiazonic acid, have been used extensively, the elegant simplicity, precision and clarity of a genetic analysis remains unparalleled. Moreover, unlike vertebrates, *Drosophila* has a single highly conserved SERCA gene making analysis of the physiological contribution of SERCA particularly feasible. Our results not only reinforce and further develop previous findings, but also open up the possibility of detailed structure-function analysis *in vivo* and screens for genetic modifiers of SERCA function.

Thus, in this report, we isolate, characterize and utilize conditional mutations in dSERCA to address specific questions about the role of SERCA-dependent calcium uptake and intra-cellular reserves of calcium in neuromuscular physiology. Using this

genetic approach, we show that 1) SERCA regulates calcium sequestration and quantal content in neurons; 2) SERCA inhibition results in altered properties of voltage-gated ion channels on plasma membrane that contribute to normal muscle firing properties; and 3) provide evidence for novel intra or intermolecular interactions that govern SERCA function *in vivo*. While some of these findings are admittedly anticipated (extensive distribution of SERCA in both neurons and muscles), others, such as the chronic regulation of ion channels by SERCA dependent mechanisms are surprisingly novel, and further refine our understanding of the role of this key protein.

SERCA regulates presynaptic calcium sequestration and quantal content:

Conditional mutant alleles of dSERCA have allowed us to analyze immediate or early effects of SERCA perturbation on the physiology of excitable cells. In both heated *CaP60A*^{Kum170} mutants and thapsigargin-treated wild-type larval motor terminals, stimulation at 30Hz, results in an unusually high initial increase in cytosolic calcium compared to a relatively modest increase in the wild type. This provides direct evidence for a SERCA-dependent mechanism in sequestering presynaptic calcium during high-frequency stimulation. Within two to four minutes of sustained 30Hz stimulation, the early calcium peak, sustained in wild-type terminals, falls in SERCA-inhibited terminals. Our data currently do not distinguish between two explanations for this phenomenon: a) that calcium entry into the nerve terminal is reduced under conditions of SERCA inhibition; or b) that release from intracellular calcium stores, not replenished during SERCA inhibition, may contribute to the initial calcium peak. More instructively, after cessation of 30Hz stimulations, intracellular calcium that remains significantly elevated

in control preparations, falls in SERCA inhibited terminals to levels below those seen in controls (Figure 4). This phenomenon is most easily explained by postulating calcium release from intracellular stores to persist after cessation of stimulation in the wild type but not in SERCA inhibited synapses in which calcium stores have been depleted. Together these data provide important genetic support for the conclusions based on pharmacological evidence that SERCA mediated calcium sequestration is operative in the pre-synaptic terminal (LAURI *et al.*; MATIAS *et al.*).

Reduced cytosolic calcium as observed in our *CaP60A*^{Kum170} mutants, might have an effect on presynaptic release properties. Our results indicate that this is indeed the case. Evoked excitatory junction potentials are reduced in heated *CaP60A*^{Kum170} animals as compared to unheated ones. Comparable heat treatment (40^{o} for five minutes, followed by recordings at room temperature) in wild type animals has negligible effects on evoked release. This suggests an effect of altered calcium sequestration (leading to the depletion of intra-cellular stores) on the probability of evoked release.

Altered synaptic transmission and membrane excitability in SERCA mutants:

The role of SERCA in calcium sequestration in muscles has been well established by several previous analyses (EAST). However, these analyses make few predictions for SERCA function in regulating membrane excitability or synaptic transmission. The importance of SERCA in cardiac dysfunction is well documented. However, the remarkable finding that SERCA potentiation can suppress multiple unrelated cardiac myopathies has not been explained at a physiological or mechanistic level. Thus, it was unexpected for us to observe failure of synaptically driven action

potentials, as well as a range of abnormalities in action-potential waveforms including slow rise time, slow decay time and abnormal spike broadening in SERCA mutants. These defects were observed in the dorsal flight muscles of adult animals that normally follow stimulation frequencies of as high as 100 Hz with high fidelity. The presence of discernible EPSPs in SERCA-inhibited muscle indicates that these defects in muscle physiology might derive primarily from alterations in the active responses of muscles to initial neurotransmitter-induced depolarization. Furthermore, strong expression of the mutant SERCA protein in muscles using the GAL4-UAS system resulted in temperature-sensitive paralysis and electrophysiological defects similar to the *CaP60A*^{Kum170} mutation. Thus, calcium sequestration by SERCA plays a critical role in maintaining the nature and fidelity of active muscle responses to synaptic stimulation.

More detailed, direct analysis of the major inward current carried by a voltage-gated calcium channel reveals that SERCA regulates the availability of voltage-gated calcium channels. *CaP60A*^{Kum170} animals on heating show a dramatic reduction in voltage-gated calcium currents. Such a reduction is likely to cause failures of muscle action potentials even at low frequencies of stimulation. At this stage we can only hypothesize about the mechanism by which there is a reduction in calcium currents. Existing data suggest a feedback inactivation of calcium channels due to initial high levels of cytosolic calcium (BURGOYNE and WEISS). There might also be additional mechanisms, e.g. kinase signaling, by which alteration of SERCA mediated calcium uptake can signal to voltage-gated channels on the cell surface and chronically attenuate calcium currents through these channels (HOEFFER *et al.*; PETERSON *et al.*; WANG *et al.*; WANG *et al.*). In this scenario, SERCA may normally function as a clamp to control

cytosolic calcium levels.

In addition to voltage-gated calcium channels, calcium-activated potassium channels also depend on SERCA function. Characteristically prolonged action potentials in *CaP60A*^{Kum170}, also observed in *slowpoke* mutants, can be explained by altered calcium-activated potassium current in these mutants (ATKINSON *et al.*). Direct measurement of the peak *slo* current shows a severely reduced calcium-activated potassium current in *CaP60A*^{Kum170} animals (Figure 8). Although our data do not provide a conclusive mechanistic explanation for the phenomenon, it is possible that the effects are a direct consequence of reduced cytosolic calcium.

At present, very little is known about how signaling pathways regulate voltage gated calcium channels or Slowpoke channels in *Drosophila*; thus, additional studies will be required to pinpoint the pathways that are involved in this process. However, our demonstration that ion-channel properties are sensitive to SERCA dysfunction provides at least one potential explanation for how a wide range of defects in cardiac physiology may be suppressed by stimulating SERCA function.

New insights into SERCA function *in vivo*:

Given that current structural models for SERCA generally consider a monomeric protein, the dominance of the conditional paralytic phenotype was surprising. It potentially indicated an unusual neomorphic (gain-of-function) effect on SERCA function. However, the remarkably similar effects of *CaP60A*^{Kum} mutations and the SERCA antagonist thapsigargin on presynaptic calcium fluxes strongly argues against this possibility. The dominant loss-of-function effect of three different dSERCA

mutations we describe, cannot be explained by haplo-insufficiency, the requirement of two wild-type alleles, because heterozygous deficiencies in this region are viable and normal. Rather the observed dominance suggests that existing structural models for SERCA should be further refined by incorporating intermolecular interactions. If SERCA exists as oligomers in the native state, then inhibiting half the SERCA molecules can have a dominant effect through the overall inhibition of all calcium transporting complexes. Given the importance of SERCA in regulation of various physiological processes, for instance, cardiac rhythm, and its relevance as a drug target (MINAMISAWA *et al.*), this is an issue of some significance.

In conclusion, we describe the effects of mutating SERCA and altering intra-cellular calcium stores on neuromuscular physiology. We demonstrate that loss-of-function mutations in dSERCA lead to conditional dominant phenotypes. We also show that SERCA regulates function of ion channels on the plasma membrane which contribute to generation and waveform of muscle action potentials. Further studies will be aimed at elucidating the link between SERCA dysfunction and ion channel modulation. Conserved signaling pathways other than direct calcium mediated feedback may also be involved in this phenomenon. Investigation of structure-function relationships of SERCA and screens to isolate modifiers of $CaP60A^{Kum170}$ are also feasible.

ACKNOWLEDGEMENTS

We wish to acknowledge members of the Ramaswami, Krishnan and Levine laboratories and Konrad Zinsmaeir for helpful comments, criticisms and suggestions. Thanks also to Carl Boswell for help with confocal imaging at the MCB confocal facility, Rene' Luedeman for help with neuronal cultures and Charles Hoeffer and Patricia Estes with western analysis and Patricia Estes for help with microinjection. CC acknowledges support from grant NS 28495 to R. Levine. Support for this work came in part from a Cancer Biology Training Grant (NIH T32 CA09213) to SS, grants from the Department of Science and Technology, Department of Biotechnology (India) and TIFR intramural funds to KSK and National Institutes of Health grants to MR (NS 34889 and DA 15485).

REFERENCES

ATKINSON, N. S., R. BRENNER, W. CHANG, J. WILBUR, J. L. LARIMER *et al.*, 2000 Molecular separation of two behavioral phenotypes by a mutation affecting the promoters of a Ca-activated K channel. J Neurosci **20:** 2988-2993.

ATKINSON, N. S., G. A. ROBERTSON and B. GANETZKY, 1991 A component of calcium-activated potassium channels encoded by the *Drosophila* slo locus. Science **253:** 551-555.

BERRIDGE, M. J., P. LIPP and M. D. BOOTMAN, 2000 The versatility and universality of calcium signalling. Nat Rev Mol Cell Biol **1:** 11-21.

BRAND, A. H., and N. PERRIMON, 1993 Targeted gene expression as a means of altering cell fates and generating dominant phenotypes. Development **118:** 401-415.

BURGOYNE, R. D., and J. L. WEISS, 2001 The neuronal calcium sensor family of Ca2+-binding proteins. Biochem J **353:** 1-12.

CATTERALL, W. A., 1999 Interactions of presynaptic Ca2+ channels and snare proteins in neurotransmitter release. Ann N Y Acad Sci **868:** 144-159.

COSTELLO, W. J., and R. J. WYMAN, 1986 Development of an indirect flight muscle in a muscle-specific mutant of *Drosophila* melanogaster. Dev Biol **118:** 247-258.

EAST, J. M., 2000 Sarco(endo)plasmic reticulum calcium pumps: recent advances in our understanding of structure/function and biology (review). Mol Membr Biol **17:** 189-200.

ELKINS, T., B. GANETZKY and C. F. WU, 1986 A *Drosophila* mutation that eliminates a calcium-dependent potassium current. Proc Natl Acad Sci U S A **83:** 8415-8419.

FABIATO, A., 1983 Calcium-induced release of calcium from the cardiac sarcoplasmic reticulum. Am J Physiol **245:** C1-14.

GIELOW, M. L., G. G. GU and S. SINGH, 1995 Resolution and pharmacological analysis of the voltage-dependent calcium channels of *Drosophila* larval muscles. J Neurosci **15:** 6085-6093.

GOMMANS, I. M., M. H. VLAK, A. DE HAAN and B. G. VAN ENGELEN, 2002 Calcium regulation and muscle disease. J Muscle Res Cell Motil **23:** 59-63.

GYORKE, S., I. GYORKE, V. LUKYANENKO, D. TERENTYEV, S. VIATCHENKO-KARPINSKI *et al.*, 2002 Regulation of sarcoplasmic reticulum calcium release by luminal calcium in cardiac muscle. Front Biosci **7:** d1454-1463.

HASSAN, B. A., N. A. BERMINGHAM, Y. HE, Y. SUN, Y. N. JAN *et al.*, 2000 atonal regulates neurite arborization but does not act as a proneural gene in the *Drosophila* brain. Neuron **25:** 549-561.

HASSELBACH, W., 1998 The Ca(2+)-ATPase of the sarcoplasmic reticulum in skeletal and cardiac muscle. An overview from the very beginning to more recent prospects. Ann N Y Acad Sci **853:** 1-8.

HOEFFER, C. A., S. SANYAL and M. RAMASWAMI, 2003 Acute induction of conserved synaptic signaling pathways in *Drosophila* melanogaster. J Neurosci **23:** 6362-6372.

IKEDA, K., and J. H. KOENIG, 1988 Morphological identification of the motor neurons innervating the dorsal longitudinal flight muscle of *Drosophila* melanogaster. J Comp Neurol **273:** 436-444.

KATZ, B., and R. MILEDI, 1969 Spontaneous and evoked activity of motor nerve endings

in calcium Ringer. J Physiol **203:** 689-706.

KING, D. G., and R. J. WYMAN, 1980 Anatomy of the giant fibre pathway in *Drosophila*. I. Three thoracic components of the pathway. J Neurocytol **9:** 753-770.

KRAFT, R., R. B. LEVINE and L. L. RESTIFO, 1998 The steroid hormone 20-hydroxyecdysone enhances neurite growth of *Drosophila* mushroom body neurons isolated during metamorphosis. J Neurosci **18:** 8886-8899.

KUROMI, H., and Y. KIDOKORO, 2002 Selective replenishment of two vesicle pools depends on the source of Ca2+ at the *Drosophila* synapse. Neuron **35:** 333-343.

LAEMMLI, U. K., and S. F. QUITTNER, 1974 Maturation of the head of bacteriophage T4. IV. The proteins of the core of the tubular polyheads and in vitro cleavage of the head proteins. Virology **62:** 483-499.

LAURI, S. E., Z. A. BORTOLOTTO, R. NISTICO, D. BLEAKMAN, P. L. ORNSTEIN *et al.*, 2003 A role for Ca2+ stores in kainate receptor-dependent synaptic facilitation and LTP at mossy fiber synapses in the hippocampus. Neuron **39:** 327-341.

LOKE, J., and D. H. MACLENNAN, 1998 Malignant hyperthermia and central core disease: disorders of Ca2+ release channels. Am J Med **104:** 470-486.

LOUGHNEY, K., R. KREBER and B. GANETZKY, 1989 Molecular analysis of the para locus, a sodium channel gene in *Drosophila*. Cell **58:** 1143-1154.

MAGYAR, A., E. BAKOS and A. VARADI, 1995 Structure and tissue-specific expression of the *Drosophila* melanogaster organellar-type Ca(2+)-ATPase gene. Biochem J **310 (Pt 3):** 757-763.

MATIAS, C., J. C. DIONISIO and M. E. QUINTA-FERREIRA, 2002 Thapsigargin blocks STP and LTP related calcium enhancements in hippocampal CA1 area. Neuroreport

13: 2577-2580.

MELZER, W., A. HERRMANN-FRANK and H. C. LUTTGAU, 1995 The role of Ca2+ ions in excitation-contraction coupling of skeletal muscle fibres. Biochim Biophys Acta **1241:** 59-116.

MINAMISAWA, S., M. HOSHIJIMA, G. CHU, C. A. WARD, K. FRANK *et al.*, 1999 Chronic phospholamban-sarcoplasmic reticulum calcium ATPase interaction is the critical calcium cycling defect in dilated cardiomyopathy. Cell **99:** 313-322.

ODERMATT, A., P. E. TASCHNER, V. K. KHANNA, H. F. BUSCH, G. KARPATI *et al.*, 1996 Mutations in the gene-encoding SERCA1, the fast-twitch skeletal muscle sarcoplasmic reticulum Ca2+ ATPase, are associated with Brody disease. Nat Genet **14:** 191-194.

PERIZ, G., and M. E. FORTINI, 1999 Ca(2+)-ATPase function is required for intracellular trafficking of the Notch receptor in *Drosophila*. Embo J **18:** 5983-5993.

PETERSON, B. Z., C. D. DEMARIA, J. P. ADELMAN and D. T. YUE, 1999 Calmodulin is the Ca2+ sensor for Ca2+ -dependent inactivation of L-type calcium channels. Neuron **22:** 549-558.

RAMASWAMI, M., S. RAO, A. VAN DER BLIEK, R. B. KELLY and K. S. KRISHNAN, 1993 Genetic studies on dynamin function in *Drosophila*. J Neurogenet **9:** 73-87.

ROBERTS, W. M., 1993 Spatial calcium buffering in saccular hair cells. Nature **363:** 74-76.

RORTH, P., 1996 A modular misexpression screen in *Drosophila* detecting tissue-specific phenotypes. Proc Natl Acad Sci U S A **93:** 12418-12422.

SANYAL, S., R. NARAYANAN, C. CONSOULAS and M. RAMASWAMI, 2003 Evidence for

cell autonomous AP1 function in regulation of *Drosophila* motor-neuron plasticity. BMC Neurosci **4:** 20.

SHENG, Z. H., R. E. WESTENBROEK and W. A. CATTERALL, 1998 Physical link and functional coupling of presynaptic calcium channels and the synaptic vesicle docking/fusion machinery. J Bioenerg Biomembr **30:** 335-345.

STEWART, B. A., H. L. ATWOOD, J. J. RENGER, J. WANG and C. F. WU, 1994 Improved stability of *Drosophila* larval neuromuscular preparations in haemolymph-like physiological solutions. J Comp Physiol [A] **175:** 179-191.

SUZUKI, N., and M. KANO, 1977 Development of action potential in larval muscle fibers in *Drosophila* melanogaster. J Cell Physiol **93:** 383-388.

THOMAS, J. B., and R. J. WYMAN, 1982 A mutation in *Drosophila* alters normal connectivity between two identified neurones. Nature **298:** 650-651.

TOYOSHIMA, C., M. NAKASAKO, H. NOMURA and H. OGAWA, 2000 Crystal structure of the calcium pump of sarcoplasmic reticulum at 2.6 A resolution. Nature **405:** 647-655.

TOYOSHIMA, C., H. NOMURA and Y. SUGITA, 2003 Structural basis of ion pumping by Ca(2+)-ATPase of sarcoplasmic reticulum. FEBS Lett **555:** 106-110.

WANG, B., C. BOLDUC and K. BECKINGHAM, 2002 Calmodulin UAS-constructs and the in vivo roles of calmodulin: analysis of a muscle-specific phenotype. Genesis **34:** 86-90.

WANG, B., K. M. SULLIVAN and K. BECKINGHAM, 2003 *Drosophila* calmodulin mutants with specific defects in the musculature or in the nervous system. Genetics **165:** 1255-1268.

FIGURE LEGENDS

Figure 1. Phenotypes associated with conditional mutations in dSERCA. (A) Both *Kum*^{170} and *Kum*^{295} are dominant temperature-sensitive paralytics and paralyze between 39^{o} and 40^{o} in three minutes. (B) Heterozygous *Kum* larvae also paralyze on heating and exhibit prolonged contraction as compared to wild type. (C) *Kum* mutations are recessively lethal. Lethal embryos appear contracted inside the egg case and fail to hatch. (D) Paralysis in *Kum* animals is dependent on neural activity. *para;Kum* animals at temperatures restrictive for both mutations, do not show the contracted phenotype. At temperatures permissive for *para*, the temperature-sensitive phenotype of *Kum* manifests itself following prior heating to restrictive temperatures.

Figure 2. *Kum* mutations map to the dSERCA locus at 60A11-12. (A) Df(2R)or-BR11 uncovers it while Df(2R)eg12 does not. The EP938 P-line was used to generate a P-element transposon tagged allele of dSERCA, *Kum*^{P52}. Plasmid rescue of this line showed the downstream gene to be dSERCA and the insertion site to be just upstream of the TATA box. Sequencing one allele, *CaP60A*^{Kum170}, from this study and an allele isolated previously, *CaP60A*^{l1}, identified the mutations in the coding region of dSERCA. (B) Fly SERCA shows a high degree of homology to vertebrate SERCA and can be homology modeled with a high degree of confidence. Shown are the sites of the mutations in *CaP60A*^{Kum170} and *CaP60A*^{l1}. Both mutations are in the "hinge" region of the molecule.

Figure 3. SERCA is highly expressed in both neurons and muscles. (A) A western blot using protein purified from adult *Drosophila* and probed with the anti-SERCA antibody. A distinct band of about 100 KDa (the predicted size from a 1003 aa protein) is recognized. The pre-immune serum and immune serum cross-adsorbed against the immunizing peptides fail to detect this band. (B) Primary neurons in culture stained with either pre-immune serum or anti-SERCA antibodies with anti-HRP as a neuronal membrane marker. The anti-SERCA antibody stains the entire neuron as compared to the pre-immune serum. (scale bar = 10 microns) (C) Staining of larval body wall with the anti-SERCA antibody shows distinct cellular compartments (possibly SER). Also seen are membranous compartments continuous with the nuclear envelope (bottom right). (D) Double staining with anti-SERCA and anti-KDEL (that labels proteins retained in the ER) shows extensive co-localization, especially in membrane continuous with the nuclear membrane. Upper panel shows a maximum projection view of a shallow stack through a body wall muscle fiber. Bottom two rows are single planes at different depths through a muscle nucleus, demonstrating a high degree of overlap. The nucleus is shown in blue for reference. (Scale bar for muscle = 100 microns; for nucleus = 25 microns).

Figure 4. *CaP60A*^{Kum170} mutants result in a loss of normal SERCA function and show elevated stimulus dependent cytosolic calcium. (A) Rhod-2-loaded boutons are electrically stimulated at 30 Hz and pseudo colored images of boutons are shown before stimulation (Pre), at about one minute (1') and four minutes (4') after the start of tetanic stimulation, and at two minutes after the end of stimulation (Post). Warmer colors correspond to higher $[Ca^{2+}]_i$. Untreated *CaP60A*^{Kum170} at 22^o (Ctrl), thapsigargin (20 uM

for 20 minutes)-treated *CaP60A*^{Kum170} at 22^{o} (+Tg) and *CaP60A*^{Kum170} at 40^{o} for 15 minutes (+heat). (B) The ordinate shows relative fluorescence increase in boutons. The resting fluorescence (Fr) was subtracted from the stimulation-induced value (Ft), and the result (ΔF=Ft-Fr) was normalized to the resting fluorescence intensity (Ft) to give ΔF/Fr x 100. The abscissa indicates the time after the start of tetanic stimulation. Fluorescence in five or three boutons was measured in one preparation. Bars above or below each value are S.E.M. The number of samples tested for each genotype and treatment are as follows; CS(-heat) 4, CS(+heat) 5, *CaP60A*^{Kum170} (-heat) 5, *CaP60A*^{Kum170} (+heat) 7 and *CaP60A*^{Kum170} (+Tg) 5.

Figure 5. Store derived calcium regulates quantal content of presynaptic release. (A) Representative traces showing reduction of mean EJC amplitude in *CaP60A*^{Kum170} following heating at 40^{0} for five minutes. The characteristics of spontaneous events remains relatively unchanged. Vertical scale bar is 10nA for EJC and 1nA for mEJC. Horizontal scale bar is 30ms for EJC and 200ms for mEJC. (B) Histograms depicting significantly reduced EJP amplitude in *CaP60A*^{Kum170} on heating ($p < 0.04$) but unaltered mEJP amplitude and frequency. All error bars are S.E.M. – indicates untreated animals and + indicates animals heated at 40^{o} for five minutes, prior to dissection and recordings at room temperature.

Figure 6. Normal SERCA function permits repetitive action potential generation: *CaP60A*^{Kum170} mutations show action potential failures. (A) Sample traces showing spontaneous activity in DLMs of unheated and heated wild type (upper traces) and

unheated and heated *CaP60A*^{Kum170} animals (lower traces). Wild type DLMs are essentially inactive with occasional bursts of firing. This pattern is unchanged on heating and is similar in unheated *CaP60A*^{Kum170} animals. However, on heating, *CaP60A*^{Kum170} animals display obvious spike broadening leading to eventual spike failure. (B) Representative traces showing that at a stimulation frequency of 30 Hz, heated *CaP60A*^{Kum170} animals exhibit spike failure before unheated *CaP60A*^{Kum170} animals while wild type animals show no failures at all. Further, spike broadening is regularly observed prior to failures in the mutants.

Figure 7. Voltage-gated calcium current in heated *CaP60A*^{Kum170} muscles are dramatically reduced. (A) Representative traces of voltage-gated calcium currents from unheated and heated wild type (top) and *CaP60A*^{Kum170} (bottom) larvae. Holding potential is –80 mV and traces corresponding to voltage steps to –20 mV through +20 mV in increments of 10 mV are shown. Voltage gated calcium currents are severely reduced in heated *CaP60A*^{Kum170} animals. (B) IV curve measuring peak barium currents through voltage-gated calcium channels in larval muscle 6 of segment A2 in unheated and heated *CaP60A*^{Kum170} animals. An IV curve from wild type animals is shown for reference (heating wild type larvae does not cause any change in the IV curve).

Figure 8. SERCA function controls action potential dynamics. (A) Representative traces from wild type and heated *CaP60A*^{Kum170} animals. Action potential failures in the *CaP60A*^{Kum170} animals are preceded by spike broadening (arrows) and multi-peaked action potentials. (B) Both the rise time and half-decay time of action potentials in heated

CaP60A^{Kum170} mutants are significantly increased as compared to wild type and unheated mutants. Histogram represents mean values obtained from several spike trains from at least 6 separate animals in each case. (C) Representative traces to show the calcium activated potassium current (slowpoke current) in heated and unheated wild type and *CaP60A*^{Kum170} larvae. Slo currents are reduced in both unheated and heated *CaP60A*^{Kum170} animals as compared to wild type. (D) Quantification of the peak slo current 10ms after the voltage step to 0mV. Measurement at this voltage step and time point gives the best estimate of the state of slo current. *CaP60A*^{Kum170} animals show minimal slo currents under these conditions.

Figure 9. Expression of dominant-negative SERCA protein in muscles is necessary and sufficient to phenocopy the *CaP60A*^{Kum170} mutation. (A) Representative traces recorded from normal and heated *Mef2-GAL4, UAS- CaP60A*^{Kum170} adults. The upper trace shows spontaneous firing in the DLMs. Like the *CaP60A*^{Kum170} mutants, action potentials show broadening with occasional failures. (B) Responses to controlled stimulation using the giant fiber pathway with and without heating. Here too, spike broadening is followed by frequent failures. This phenotype is exacerbated in response to heating as expected from the conditional nature of the mutation.

TABLE I

Expression of mutant *CaP60A*^{Kum170} in muscles is necessary and sufficient to phenocopy the *CaP60A*^{Kum170} mutation.

Genotype	Larval Paralysis	Adult Paralysis
CaP60A^{Kum170}	+++	+++
Neural		
C155	--	--
Cha	--	--
C380	--	--
Ubiquitous		
Armadillo	--	--
Shibire	--	--
Tubulin	++	--
Muscle		
MHC	+	--
24B	++	--
Mef2	+++	++

Overexpression of the mutant *CaP60A*^{Kum170} protein in muscles mimics the *CaP60A*^{Kum170} mutant

phenotypes. Expression in neural tissue does not lead to any observable paralysis. Adult and larval paralysis are compared to that in *CaP60A*^{Kum170} animals incubated at the restrictive temperature of 40^{o} for three minutes.

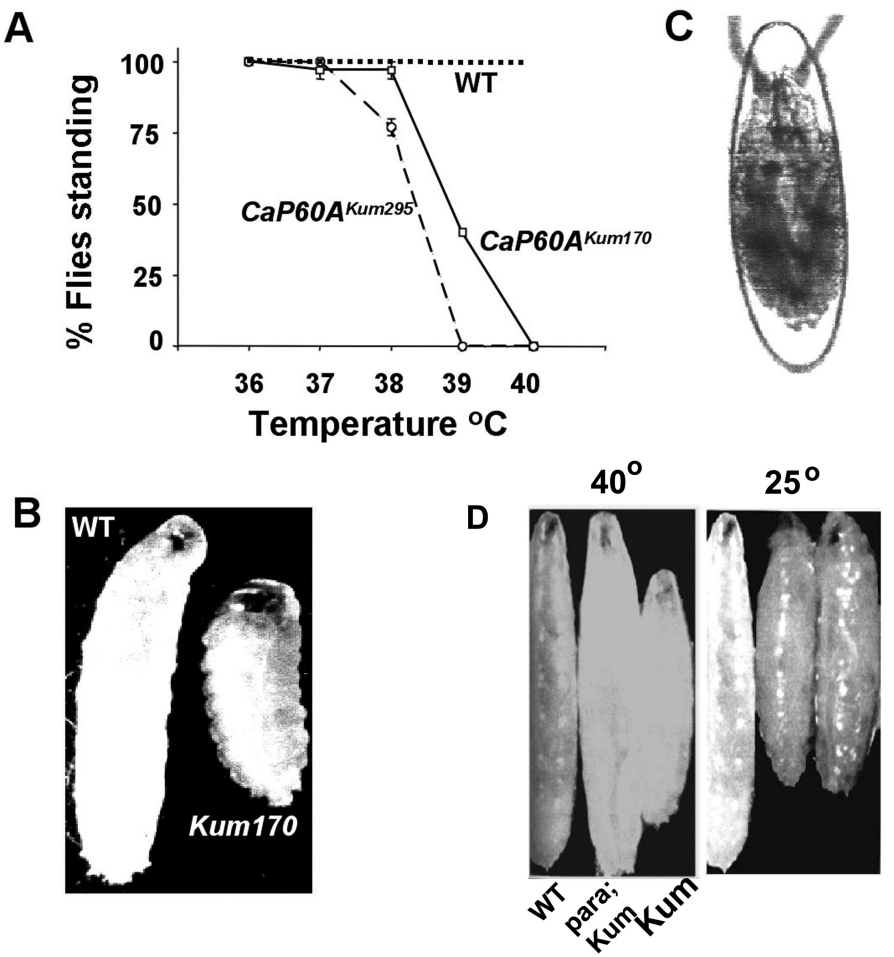
A
100
75
50
25
0
% Flies standing
WT
CaP60A Kum295
CaP60A Kum170
36
37
38
39
40
Temperature °C
C
B
WT
Kum170
D
40°
25°
WT
para; Kum
Kum

Figure 1

A

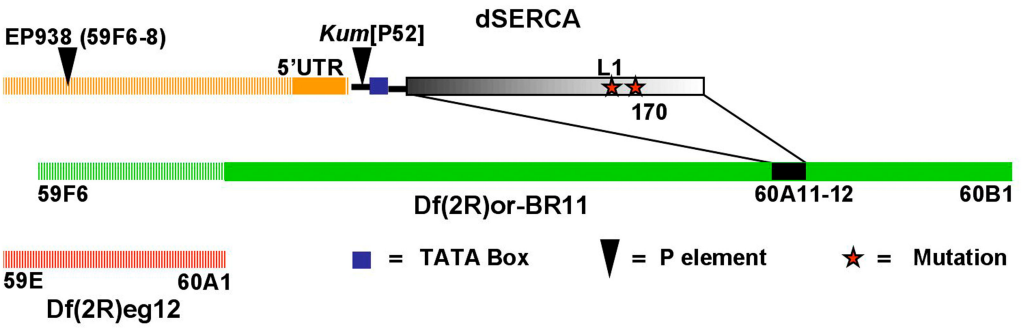
EP938 (59F6-8)
Kum[P52]
dSERCA
5'UTR
L1
170
59F6
Df(2R)or-BR11
60A11-12
60B1
59E
60A1
Df(2R)eg12
= TATA Box
= P element
= Mutation

B

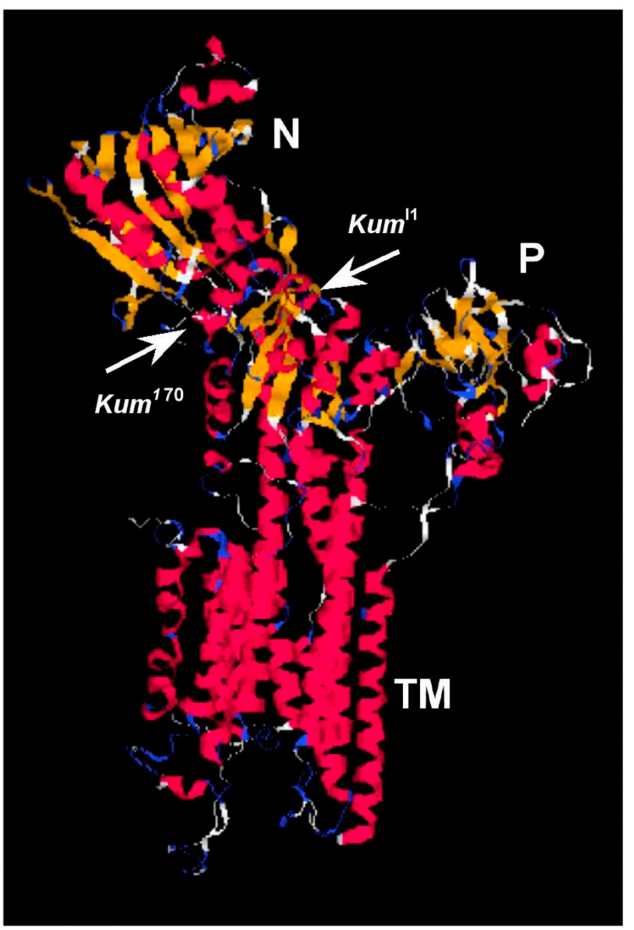
N
Kum l1
P
Kum 170
TM

Figure 2

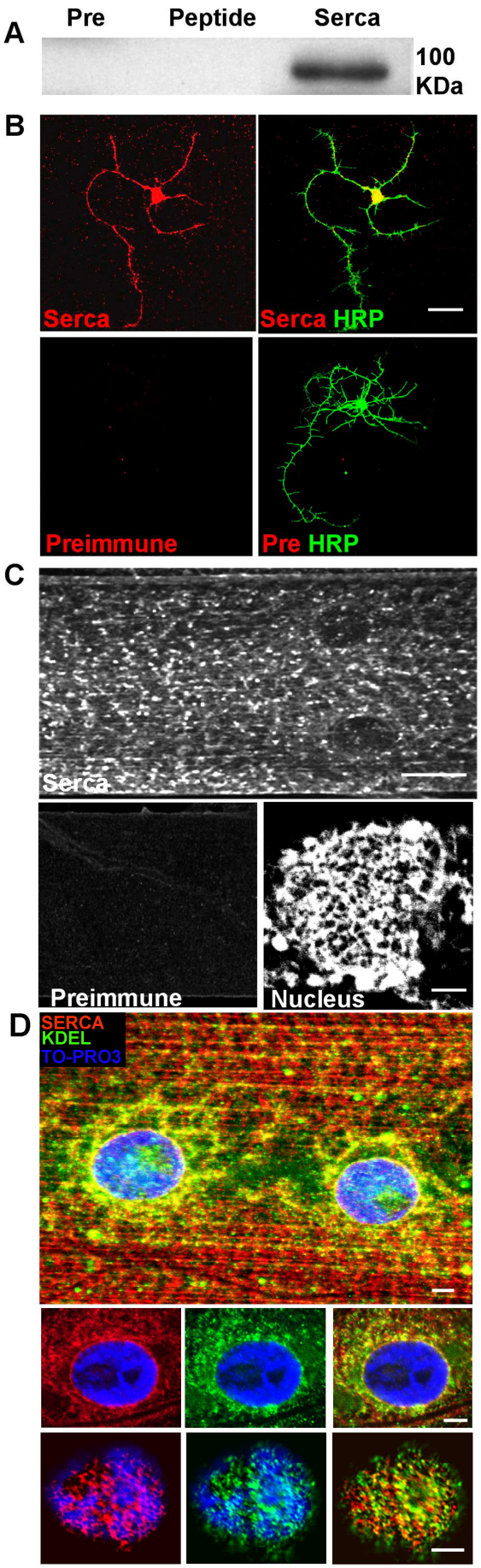
A
Pre
Peptide
Serca
100
KDa
B
Serca
Serca HRP
Preimmune
Pre HRP
C
Serca
Preimmune
Nucleus
D
SERCA
KDEL
TO-PRO3

Figure 3

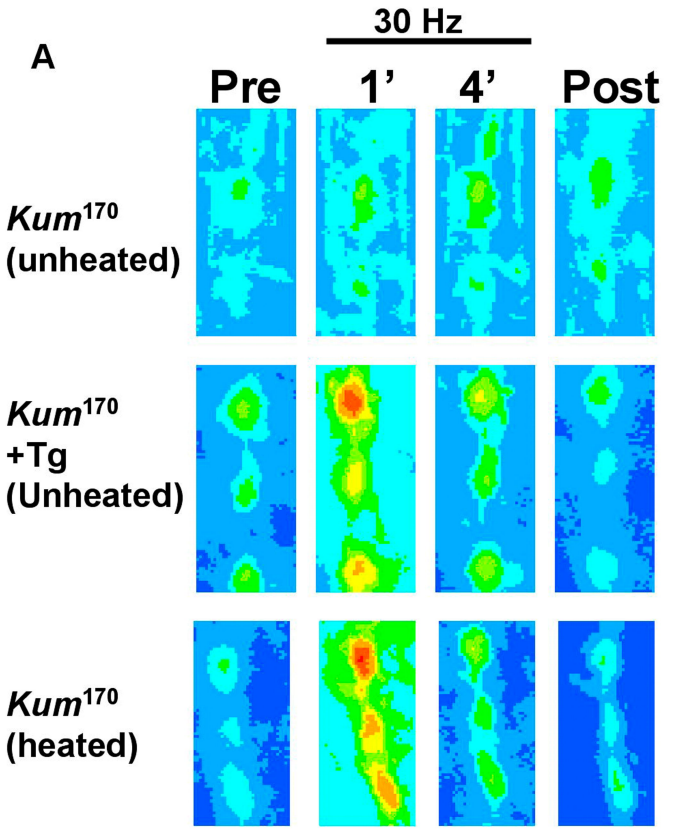
A
30 Hz
Pre
1'
4'
Post
Kum170
(unheated)
Kum170
+Tg
(Unheated)
Kum170
(heated)

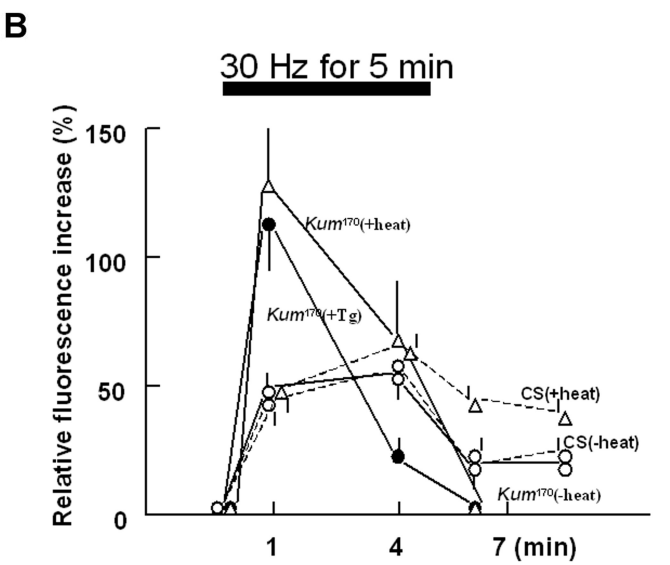
B
30 Hz for 5 min
Relative fluorescence increase (%)
150
100
50
0
Kum170(+heat)
Kum170(+Tg)
CS(+heat)
CS(-heat)
Kum170(-heat)
1
4
7 (min)

Figure 4

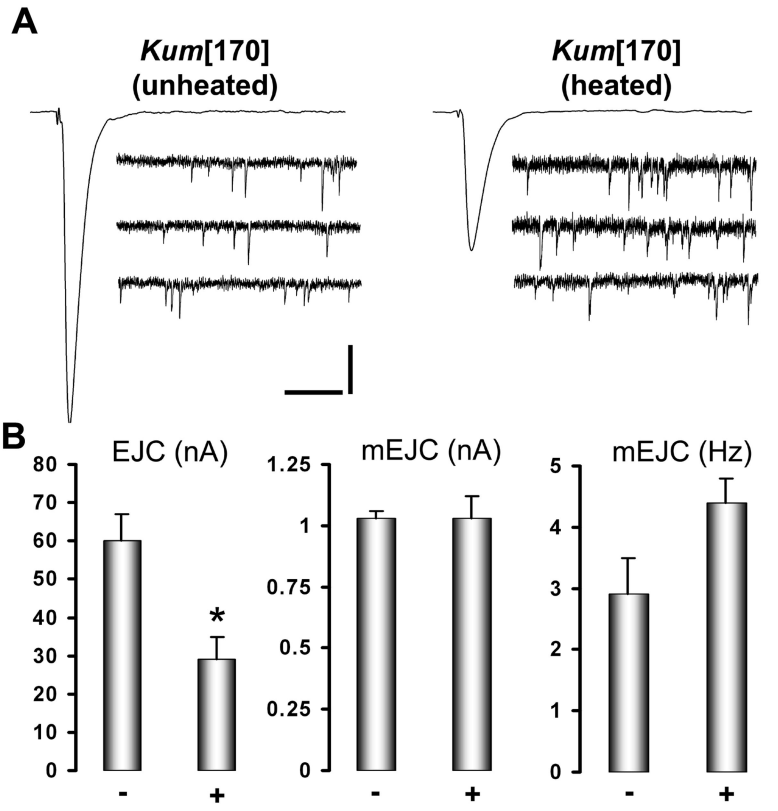
A
Kum[170]
(unheated)
Kum[170]
(heated)
B
EJC (nA)
mEJC (nA)
mEJC (Hz)
80
70
60
50
40
30
20
10
0
*
1.25
1
0.75
0.5
0.25
0
5
4
3
2
1
0
-
+
-
+
-
+

Figure 5

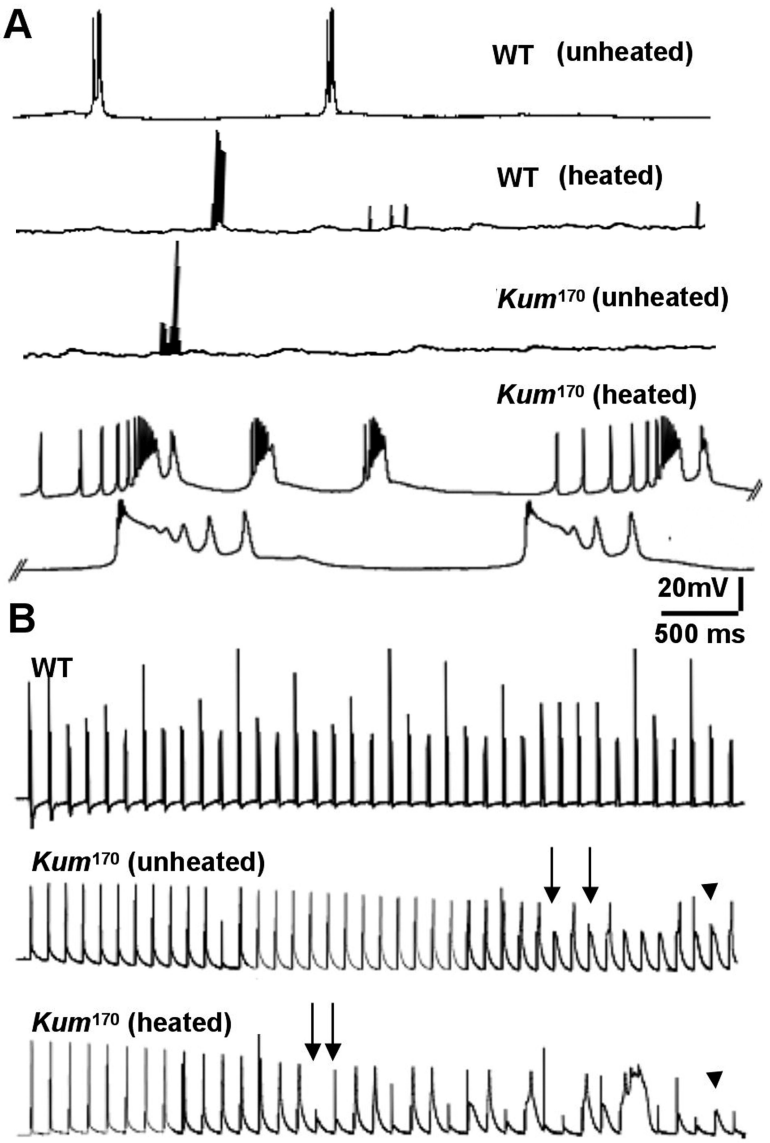
A
WT (unheated)
WT (heated)
Kum170 (unheated)
Kum170 (heated)
20mV
500 ms
B
WT
Kum170 (unheated)
Kum170 (heated)

Figure 6

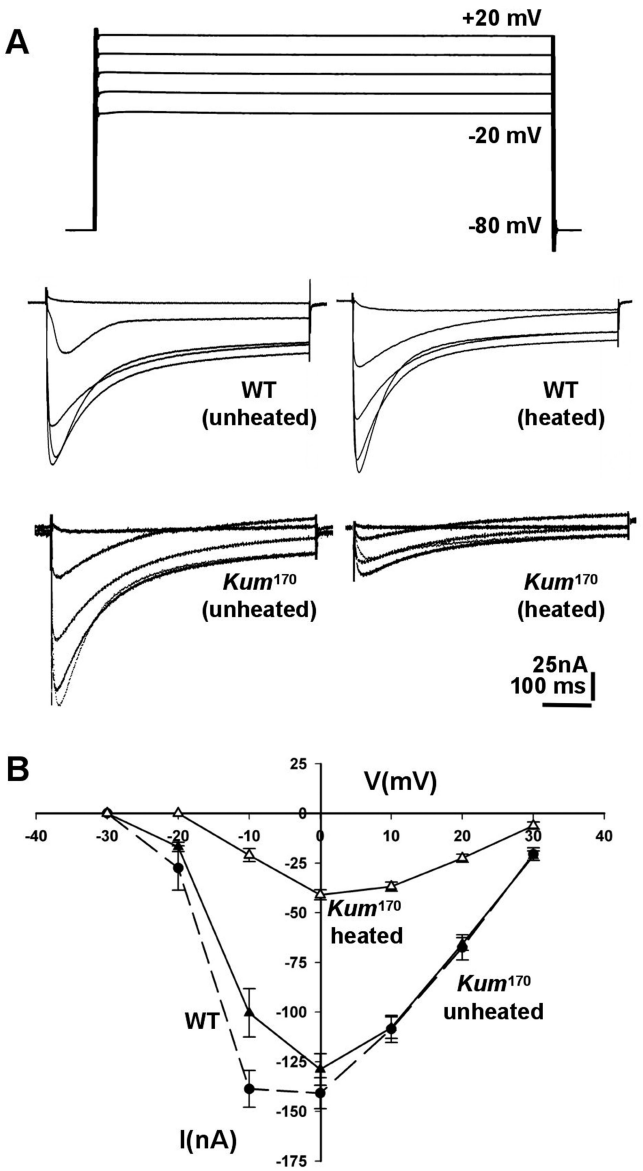
A
+20 mV
-20 mV
-80 mV
WT
(unheated)
WT
(heated)
Kum170
(unheated)
Kum170
(heated)
25nA
100 ms
B
V(mV)
I(nA)
Kum170
heated
Kum170
unheated
WT

Figure 7

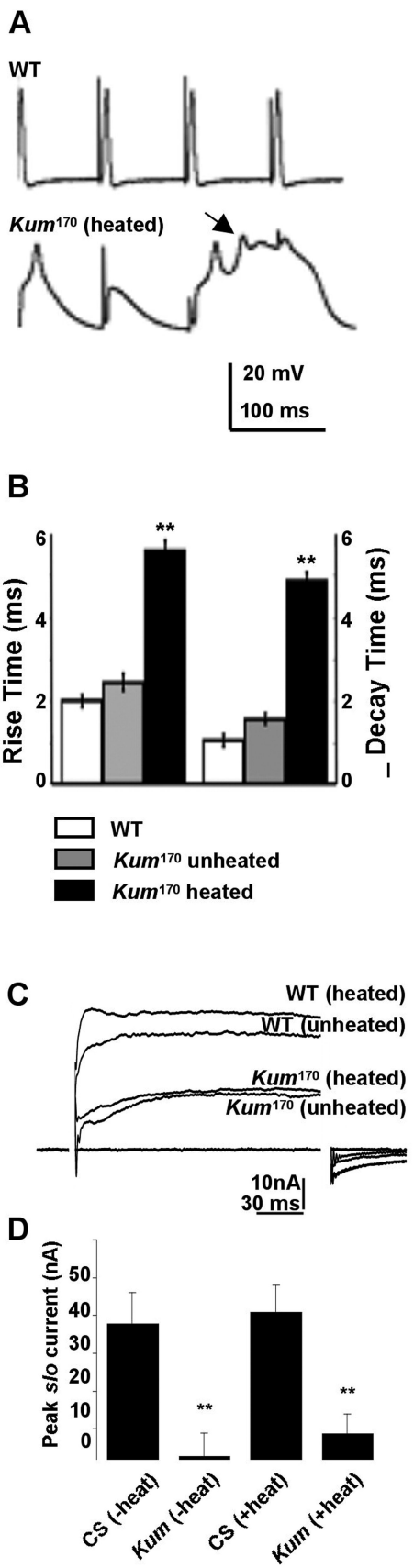
A
WT
Kum170 (heated)
20 mV
100 ms
B
Rise Time (ms)
Decay Time (ms)
0
2
4
6
**
**
WT
Kum170 unheated
Kum170 heated
C
WT (heated)
WT (unheated)
Kum170 (heated)
Kum170 (unheated)
10nA
30 ms
D
Peak slo current (nA)
0
10
20
30
40
50
**
**
CS (-heat)
Kum (-heat)
CS (+heat)
Kum (+heat)

Figure 8

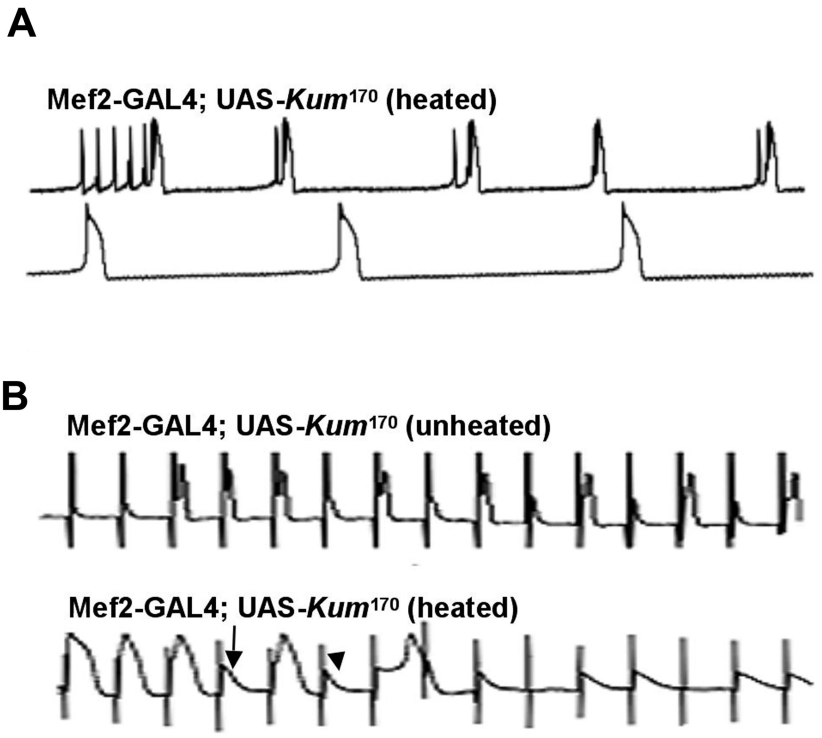
A
Mef2-GAL4; UAS-*Kum*^{170} (heated)
B
Mef2-GAL4; UAS-*Kum*^{170} (unheated)
Mef2-GAL4; UAS-*Kum*^{170} (heated)

Figure 9